

Titre: Title:	Longitudinal Flight Control Design with Handling Quality Requirements
Auteurs: Authors:	David Saussié, Ouassima Akhrif and Lahcen Saydy
Date:	2005
Type:	Rapport / Report
Référence: Citation:	Saussié, David, Akhrif, Ouassima et Saydy, Lahcen (2005). Longitudinal Flight Control Design with Handling Quality Requirements. Rapport technique. EPM-RT-2005-01.



Document en libre accès dans PolyPublie

Open Access document in PolyPublie

URL de PolyPublie: PolyPublie URL:	http://publications.polymtl.ca/2618/
Version:	Version officielle de l'éditeur / Published version Non révisé par les pairs / Unrefereed
Conditions d'utilisation: Terms of Use:	Autre / Other



Document publié chez l'éditeur officiel

Document issued by the official publisher

Maison d'édition: Publisher:	École Polytechnique de Montréal
URL officiel: Official URL:	http://publications.polymtl.ca/2618/
Mention légale: Legal notice:	Tous droits réservés / All rights reserved

**Ce fichier a été téléchargé à partir de PolyPublie,
le dépôt institutionnel de Polytechnique Montréal**

This file has been downloaded from PolyPublie, the
institutional repository of Polytechnique Montréal

<http://publications.polymtl.ca>

EPM-RT-2005-01

**LONGITUDINAL FLIGHT CONTROL DESIGN WITH
HANDLING QUALITY REQUIREMENTS**

David Saussié, Ouassima Akhrif, Lahcen Saydy
Département de Génie électrique
École Polytechnique de Montréal

Janvier 2005

Poly

EPM-RT-2005-01

LONGITUDINAL FLIGHT CONTROL DESIGN WITH
HANDLING QUALITY REQUIREMENTS

David Saussié
Ouassima Akhrif
Lahcen Saydy
École Polytechnique de Montréal et
École de Technologie Supérieure

Janvier 2005

©2005
David Saussié, Ouassima Akhrif, Lahcen Saydy
Tous droits réservés

Dépôt légal :
Bibliothèque nationale du Québec, 2005
Bibliothèque nationale du Canada, 2005

EPM-RT-2005-01

Longitudinal Flight Control Design with Handling Quality Requirements

par : David Saussié, Ouassima Akhrif, Lahcen Saydy

Département de génie électrique.

École Polytechnique de Montréal et École de Technologie Supérieure

Toute reproduction de ce document à des fins d'étude personnelle ou de recherche est autorisée à la condition que la citation ci-dessus y soit mentionnée.

Tout autre usage doit faire l'objet d'une autorisation écrite des auteurs. Les demandes peuvent être adressées directement aux auteurs (consulter le bottin sur le site <http://www.polymtl.ca/>) ou par l'entremise de la Bibliothèque :

École Polytechnique de Montréal
Bibliothèque – Service de fourniture de documents
Case postale 6079, Succursale «Centre-Ville»
Montréal (Québec)
Canada H3C 3A7

Téléphone : (514) 340-4846
Télécopie : (514) 340-4026
Courrier électronique : biblio.sfd@courriel.polymtl.ca

Ce rapport technique peut-être repéré par auteur et par titre dans le catalogue de la Bibliothèque :
<http://www.polymtl.ca/biblio/catalogue.htm>

Longitudinal flight control design with handling quality requirements

D. Saussié

Department of Electrical Engineering
École Polytechnique de Montréal
Montréal, CA

L. Saydy

Department of Electrical Engineering
École Polytechnique de Montréal
Montréal, CA

O. Akhrif

Department of Electrical Engineering
École de Technologie Supérieure
Montréal, CA

ABSTRACT

This work presents a method for selecting the gain parameters of a C^* control law for an aircraft's longitudinal motion. The design incorporates various handling quality requirements involving modal, time- and frequency-domain criteria that were fixed by the aircraft manufacturer. After necessary model order-reductions, the design proceeds in essentially two-steps: Stability Augmentation System (SAS) loop design and Control Augmentation System (CAS) loop design. The approach partly relies on the use of guardian maps to characterize, in each case, the set of gain parameters for which desired handling quality requirements are satisfied. The approach is applied throughout the full flight envelope of a business jet aircraft and yields satisfactory results.

NOMENCLATURE

\mathbb{C}	Set of complex numbers
\mathbb{C}_-^0	Open left complex half-plane
C^*	C-star mixed output
n_z	normal load factor
q	pitch rate
$\mathbb{R}^{n \times n}$	Set of $n \times n$ real matrices
u	axial velocity perturbation
w	normal velocity perturbation
α	incidence
γ	flight path angle
x_5	tail downwash angle
θ	pitch attitude
ω_{ph}	phugoid undamped natural frequency
ω_{sp}	short period mode undamped natural frequency
ζ_{ph}	phugoid damping ratio
ζ_{sp}	short period mode damping ratio

Abbreviations

CAP Control Anticipation Parameter

CAS Control Augmentation System

GUI Graphical User Interface
HQ Handling Quality
PIO Pilot-Induced Oscillation
SAS Stability Augmentation System

1.0 INTRODUCTION

Because of stringent performance and robustness requirements, modern control techniques are well suited to the design of new flight control systems. However, their complexity can prevent them from being directly implemented. The present article built on the work initiated by Saydy *et al*⁽¹⁾ proposes guidelines for choosing the gains of a classical C^* control law⁽²⁻⁴⁾ for a longitudinal flight control system of a business jet aircraft. The technique relies in part on Guardian Maps⁽⁵⁾.

The proposed C^* controller has a fixed architecture and the controller gains are adjusted in order to fulfil the desired requirements which include satisfying certain handling qualities, an important issue in modern flight control systems⁽⁶⁻¹¹⁾. Handling qualities (HQs) can be divided in three categories: modal, frequency and temporal criteria. While some of these criteria can be satisfied more easily than others, one has to deal with all three categories in control design. The approach presented in this article focuses on finding sets of feasible controller gains, i.e gains which ensure the satisfaction of the desired HQ requirements. Two additional objectives which are tackled using the same methodology, though not reported on here, are the gain-scheduling and the robustness issues (work on the latter two aspects will be presented elsewhere).

The theory of guardian maps deals with the robust generalized stability of families of parameterized linear systems. Generalized stability deals with the confinement of system poles to general regions of the complex plane of which the left half plane and the open unit disk are the two traditional examples. In robustness studies, the parameters are uncertain parameters. In the present work, the parameters are taken to be the

controller gains. A multivariable polynomial in the gains is obtained with the property that any set of gains for which this polynomial is positive is guaranteed to satisfy certain HQ requirement, i.e. to place the closed-loop poles in a desired HQ region. This condition may also be used in a constrained optimization setup to further seek controller gains that improve the tracking of a desired time-response by the output of the closed-loop system.

The design approach is based upon the natural separation of the two control loops, the inner loop called SAS (Stability Augmentation System) and the outer loop called CAS (Control Augmentation System). First, an open-loop order reduction is performed to design the SAS using guardian maps and to find gain sets that improve pole damping. Then, the CAS is tuned in order to fulfil all the remaining criteria and to improve performance. A GUI was developed to assist the designer in carrying out these steps.

Section 2 presents the C^* controller and the open-loop description. Section 3 reviews the handling qualities of interest. Section 4 provides a quick overview of Guardian Maps. Section 5 develops the methodology itself as it applies to a business jet aircraft, the data of which was provided by *Bombardier Aerospace Inc.*

2.0 Flight control system architecture

The open loop and the flight control system architecture are now briefly described.

2.1 The open loop

The open loop consists of the actuator, the aircraft dynamics and the sensors. Even though the numerical data used in this paper corresponded to a particular business jet model, the results apply to other aircraft models as well.

Supprimé : if

2.1.1 Aircraft dynamics

All models considered are linearized around flight conditions (fixed Mach number and altitude) defined by the aircraft flight envelope. These are 5th order state space models instead of the usual 4th order ones found in the literature⁽¹²⁻¹⁴⁾ The fifth state in our models, denoted x_5 , is the tail downwash angle. The generic form is:

$$\begin{cases} \dot{\mathbf{x}} = A\mathbf{x} + B\delta_e \\ \mathbf{y} = C\mathbf{x} + D\delta_e \end{cases} \quad \dots(1)$$

where the state vector is:

$$\mathbf{x} = [u \quad w \quad q \quad \theta \quad x_5]^T \quad \dots(2)$$

The input is the elevator angle δ_e and the output vector is

$$\mathbf{y} = [q \quad n_z]^T \quad \dots(3)$$

The usual pole configuration (short-period and phugoid modes) is unaffected by the presence of the fifth state as it only introduces a fifth fast and real pole which does not significantly influence the aircraft behaviour (Fig. 1).

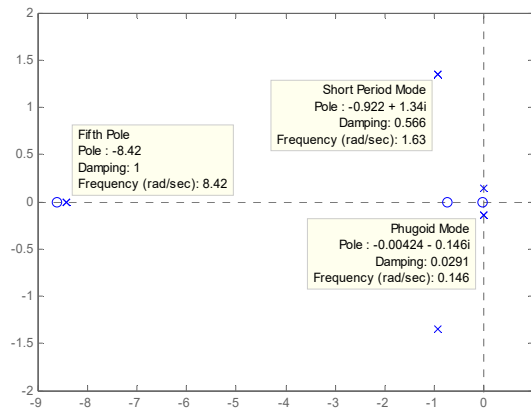


Figure 1. Pole-zero map of θ/δ_e

2.1.2 Actuator and IRU sensors

Due to the presence of delays in the actuator dynamics, the actuator model is a 15th order transfer function when the time delays are each approximated by a 5th order transfer functions. In the [0-20] (rad/s) bandwidth. However, the actuator is practically a first order filter. Thus at the control design stage only the dominant pole is kept for lower frequency reduction. For closed-loop simulations, the entire 15th order dynamics will be considered.

Similarly to the actuator, the sensor dynamics are modelled as a 15th order system but at low frequency it can be considered to be a pure gain.

Supprimé : is

2.2 C* control

The C* control law was first developed by NASA during a study for the Space Shuttle. It was then used in 1978 on the Concorde and proved its efficiency⁽¹⁵⁾. The so-called C* parameter is a mixed output of the (filtered) load factor n_{zf} and the pitch rate q (Fig. 2):

$$C^* = n_z + 12.4q \quad \dots(4)$$

The 12.4 weighting between the two outputs is the one usually used. See Field⁽¹⁶⁾ for further explanations about the 12.4 weighting value.

The control system is divided into two control loops (Fig. 2). The SAS inner loop is a dynamic feedback of the measured pitch rate via a *Wash-Out* filter. At low frequencies, the filter differentiates the signal and behaves like static feedback at high frequencies. The filter pole $-z_{wo}$ and the gain K_q are parameters to be adjusted.

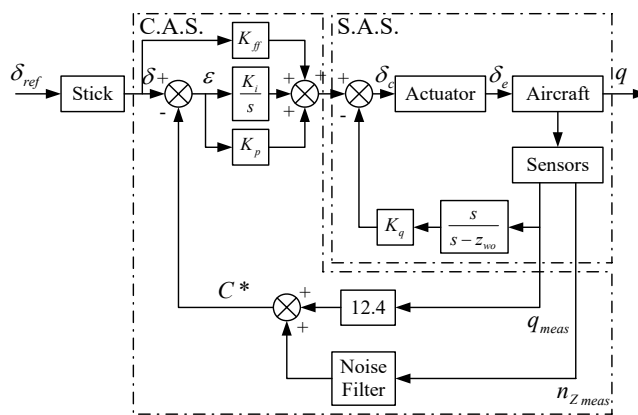


Figure 2. C^* control law

The CAS outer loop consists of the feedback of the mixed output C^* . Before combining the measured n_z and q outputs, the load factor is first passed through a filter to prevent high frequency noise corruption. The error difference between the pilot command δ and the C^* output is fed to a PI controller with gains K_p and K_i that

Supprimé : which
Supprimé : are to

can be adjusted. A feedforward gain K_{ff} completes the loop and adds some phase by tuning one system zero. Therefore, four gains (K_q, K_p, K_i, K_{ff}) and one pole ($-z_{wo}$) must be tuned in order to satisfy all the handling qualities.

3.0 HANDLING QUALITIES

The overall performance objective is to track pitch-rate commands with predicted Level 1 HQs and desired time-domain response behaviour. We will present in this section, the different handling qualities that need to be satisfied. For more on the subject one may consult Hodgkinson⁽⁷⁾. Several quantitative HQ criteria are considered in the present article. The boundary limits of these criteria are defined by military standards⁽¹⁷⁾. The different handling qualities will first be introduced, then the boundaries that must be fulfilled are presented.

3.1 Modal criteria

The criteria introduced here deal essentially with the damping ratios of the aircraft natural modes: the Phugoid and the Short Period modes. The Control Anticipation Parameter (CAP) is an additional criterion blending the natural Short Period frequency and the corresponding zero.

3.1.1 Phugoid and short period modes

The low frequency oscillating Phugoid mode is generally underdamped. It mainly affects pitch attitude θ , relative speed u , altitude h and flight path γ , whereas angle of attack α remains relatively constant. The Phugoid mode constraints are not particularly stringent as, in order to be Level 1, the Phugoid damping ratio must merely be greater than 0.04.

The Short Period mode, a rapid, oscillating mode, mostly affects the transient responses in angle of attack α , pitch rate q and load factor n_z . Forward relative speed remains practically unaffected by its oscillations.

Supprimé : Contrary to

Supprimé : important

Compared with the Phugoid mode, the Short Period mode constraints are more stringent. To be Level 1, the damping ratio must be between 0.35 and 1.30.

3.1.2 Control anticipation parameter

As the short period motion is affected both by the Short Period mode and the numerator of the corresponding transfer functions, the numerator effect has been incorporated in a criterion called Control Anticipation Parameter (CAP). By definition, it is the ratio of the initial pitch acceleration to the final normal acceleration:

$$CAP = \frac{\ddot{\theta}_0}{\Delta n_z} \approx \frac{\omega_{SP}^2}{U_0} \frac{1}{g T_\theta} \quad \dots(5)$$

where ω_{SP} is the Short Period natural frequency, U_0 the trimming speed, g the acceleration of gravity and T_θ the short period numerator time constant in the q/δ aircraft longitudinal transfer function.

The CAP amplitude gives a good indication about the pilot's perception of the pitch and vertical accelerations.

Fig. 3 shows the limitations on CAP and how they relate to the Short Period damping criteria⁽¹⁷⁾. This criterion would not however, be among the handling qualities we will try to satisfy with the guidelines. Its value will be checked after the design, to ensure it is within the boundaries.

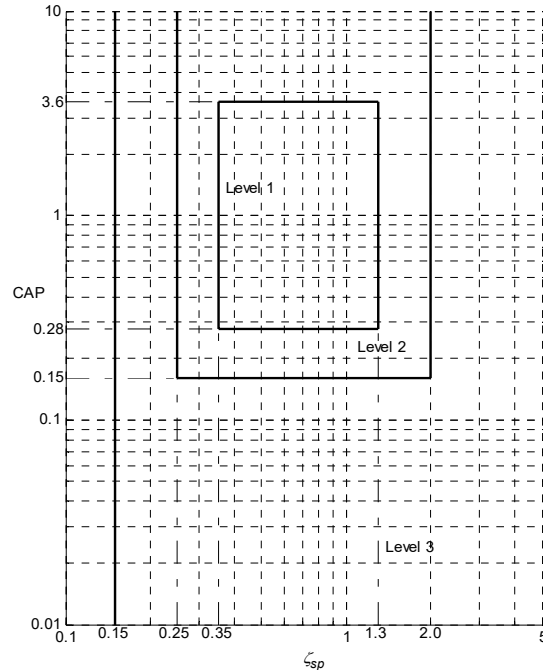


Figure 3. CAP Limitations

3.2 Frequency criteria

Frequency criteria are all calculated using the high-order model. Both θ -Bandwidth and γ -Bandwidth are criteria for pilot-in-the-loop analysis where the pilot model is represented by a simple gain. From the frequency response of the considered output to stick input, the bandwidth frequency is the lower frequency of

Supprimé : smaller

the one for which the phase angle is -135° , $\omega_{BW\phi}$, and the one which the gain margin is 6 dB, ω_{BWG} . The phase delay τ_p is the relative phase variation between ω_{180° and $2\omega_{180^\circ}$:

$$\tau_p = \frac{\pi}{180} \cdot \frac{\Delta\Phi}{2\omega_{180^\circ}} \quad \dots(6)$$

Fig. 4 illustrates how to calculate these.

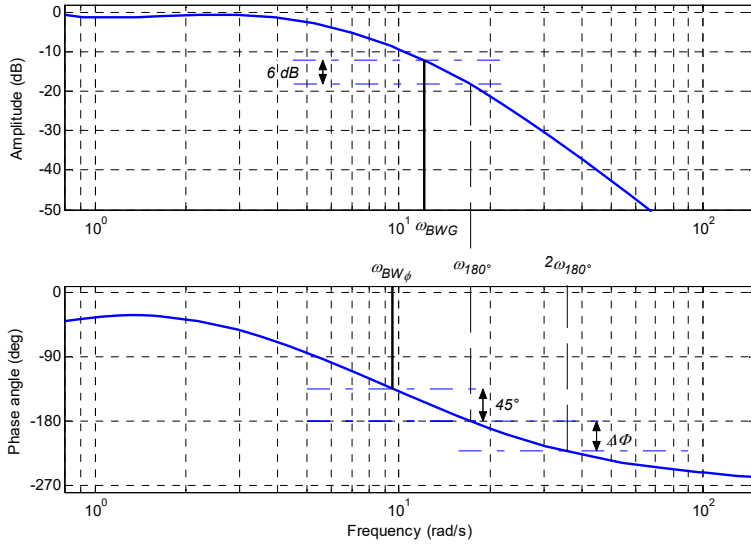


Figure 4. Definition of bandwidth

θ -bandwidth and Phase Delay are both calculated based on the θ/δ_{ref} transfer function (Fig. 1) and γ -bandwidth on the γ/δ_{ref} transfer function. Note that for the latter, the bandwidth is $\omega_{BW\phi}$. For detailed graphs and boundaries, see Hodgkinson⁽⁷⁾ or military standards⁽¹⁷⁾.

The gain and phase margins are the ones of the CAS loop, in this case C^*/ε . These margins are linked to the robustness of the closed loop in classical control design.

3.3 Time-domain criteria and Gibson dropback

Supprimé : rising

Besides the classical time-domain criteria such as settling time, overshoot or rise time, Gibson dropback is commonly used by flight control engineers. It is a short term measure of the pitch attitude changes and it is calculated based on the reduced-order attitude θ response (i.e. without the Phugoid mode) to a stick step input. Figure 5 illustrates how to calculate the dropback Drb . The quantity q_{ss} is the pitch rate steady state value. The resulting expression remains valid as long as the settling time is satisfactory.

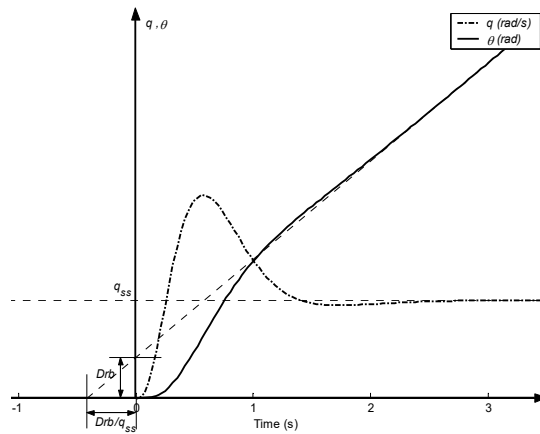


Figure 5. Dropback definition

A general theoretical formula for the dropback in terms of system parameters was obtained by the authors and is given next. The details of the proof are provided in (3). For the proper transfer function given by:

$$\frac{q}{\delta_{ref}} = K \frac{\prod_{i=1}^k (1 + T_i s) \prod_{i=1}^l (s^2 + 2\xi_i \phi_i s + \phi_i^2)}{\prod_{i=1}^m (1 + \tau_i s) \prod_{i=1}^n (s^2 + 2\zeta_i \omega_i s + \omega_i^2)} \quad \dots(7)$$

the expression of the dropback is:

$$\frac{Drb}{q_{ss}} = \left(\sum_{j=1}^k T_i + \sum_{j=1}^l 2 \frac{\zeta_i}{\phi_j} \right) - \left(\sum_{j=1}^m \tau_i + \sum_{j=1}^n 2 \frac{\zeta_i}{\omega_j} \right) \dots(8)$$

Note that the dropback is independent of K . If the expanded formulation is used for the transfer function:

$$\frac{q}{\delta_{ref}} = \frac{a_0 + a_1s + a_2s^2 + \dots}{b_0 + b_1s + b_2s^2 + \dots}, \dots(9)$$

then :

$$\frac{Drb}{q_{ss}} = \frac{a_1}{a_0} - \frac{b_1}{b_0} \dots(10)$$

This formula will be useful when expressing the dropback as a function of the various controller gains.

3.4 HQ Boundaries

Table 1 summarizes the boundaries of the handling qualities that must be Level 1. In this application, the more stringent ‘Good Level 1’ boundaries are used⁽⁶⁾.

Table 1. Handling quality boundaries

HQs	Level 1	Good Level 1
Short Period ζ_{sp}	$0.35 < \zeta_{sp} < 1.35$	$0.7 < \zeta_{sp} < 1.35$
θ -bandwidth $\omega_{BW\theta}$	> 1.5 (rad/s)	> 1.75 (rad/s)
γ -bandwidth $\omega_{BW\gamma}$	> 0.6 (rad/s)	
Phase Delay τ_p	< 0.2 (s)	< 0.14 (s)
Gibson Dropback Drb	$-0.2 < Drb < 0.5$	$0.0 < Drb < 0.3$

Gain Margin M_G	>6 (dB)	
Phase Margin M_ϕ	>45 (°)	
Settling Time ST	2% within 3 (s)	1% within 3 (s)

4.0 GUARDIAN MAPS AND ROBUST STABILITY

The guardian map approach was introduced by Saydy and al.⁽⁵⁾ as a unifying tool for the study of generalized stability of parameterized families of matrices or polynomials. Here, generalized stability means confinement of matrix eigenvalues or polynomial zeros to general open subsets of the complex plane and includes the open left-half plane and the unit circle as special cases. Practical considerations relating to damping ratio, bandwidths etc. are commonly expressed in terms of the generalized stability formulation, with respect to a suitable domain Ω in the complex plane. Some of the basic concepts are introduced.

4.1 Guardian maps

Basically, guardian maps are scalar valued maps defined on the set of $n \times n$ real matrices (or n^{th} order real polynomials) that take non-zero values on the set of “stable” matrices (or polynomials) and vanish on its boundary. The description below will focus on families of matrices with the understanding that it applies to polynomials as well. We are hence interested in stability sets of the form:

$$S(\Omega) = \{A \in \mathbb{R}^{n \times n} : \sigma(A) \subset \Omega\} \quad \dots(11)$$

were Ω is an open subset of the complex plane of interest, and $\sigma(A)$ denotes the set consisting of all the eigenvalues of A . Such sets $S(\Omega)$ will be referred to as *generalized stability sets*, and thus represent the set of all matrices which are stable relative to Ω , i.e. which have all their eigenvalues in Ω .

Definition 1 Let ν map $\mathbb{C}^{n \times n}$ into \mathbb{C} . We say that ν guards $S(\Omega)$ if for all $A \in \overline{S}(\Omega)$, the following equivalence holds:

$$\nu(A) = 0 \Leftrightarrow A \in \overline{S}(\Omega) \quad \dots(12)$$

Here \overline{S} denotes closure of the set S . The map is said to be *polynomial* if it is a polynomial function of the entries of its argument.

Example 1: Hurwitz Stability

The open left complex half-plane, \mathbb{C}_-^0 is guarded by:

$$\nu(A) = \det(A \circ I) \det A \quad \dots(13)$$

where \circ denotes the bialternate product, in the case of matrices⁽⁴⁾.

4.2 Robust stability

The robust stability problem for parameterized families of matrices or polynomials may be stated as follows.

Let $\{A(r) : r \in U \subset \mathbb{C}^k\}$ be a continuous family of $n \times n$ matrices which depend on the uncertain parameter

vector $r := (r_1, \dots, r_k)$ where each parameter lies in a given range for which only the bounds are known, say

$r \in U \subset \mathbb{C}^k$. Assume the family is nominally stable relative to a given region of interest Ω of the complex

Supprimé : $\mathbb{R}^{n \times n}$

Supprimé :

Supprimé : \mathbb{C}

plane; i.e. $A(r^0)$ has all its eigenvalues in Ω for a given r^0 in U (simply written $A(r^0) \in S(\Omega)$). The basic question in robust stability is the following: As the parameter values are uncertain, do the eigenvalues of $A(r)$ remain confined to Ω or not? In other words, does $A(r) \in S(\Omega)$ for all $r \in U$?

The next theorem gives a basic necessary and sufficient condition for this problem.

Theorem 1 Let $S(\Omega)$ be guarded by the map v . The family $\{A(r): r \in U\}$ is stable relative to Ω if and only if

(i) it is nominally stable, i.e. $A(r^0) \in S(\Omega)$ for some $r^0 \in U$; and,

(ii) $v(A(r)) \neq 0$, for all $r \in U$.

Example 2:

The state space matrix

$$A(r) = \begin{bmatrix} -1 + 2r_1 - r_1^2 - r_2^2 & 1 + r_1 - r_1^2 - r_2^2 \\ 1 - 4r_1 + 2r_1^2 + 2r_2^2 & -3 - 2r_1 + 2r_1^2 + 2r_2^2 \end{bmatrix}$$

where $r_1, r_2 \in [-1, 1]$ is nominally (Hurwitz) stable for $r_1^0 = r_2^0 = 0$. Using the expression in Example 1, one

finds that $v(A(r)) = (r_1^2 + r_2^2 - 4)(2 - r_1)$. Since this does not vanish in $U = [-1, 1] \times [-1, 1]$, we conclude from

Theorem 1 that we have robust stability.

4.3 Gain Characterization

In our present study, the parameters are the controller gains and we seek to characterize whole regions of the gains such that the corresponding closed-loop poles all lie within a given region Ω of the complex plane. For Ω equal to the open left-hand plane, this would coincide with the set of stabilizing gains. To do so, we will rely on a corollary of the Theorem as shown below.

Supprimé : <sp>

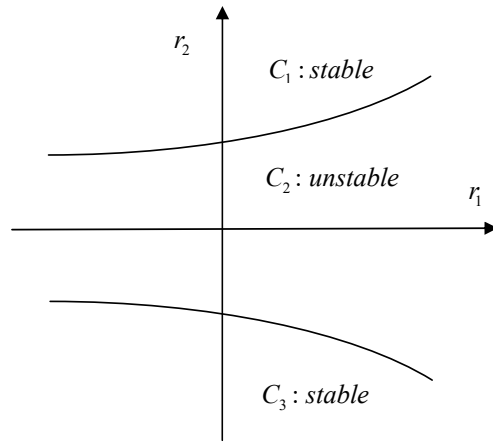


Figure 6. Example of a component corollary application

Figure 6 illustrates the corollary for a two-parameter case.

Corollary 1. Let $S(\Omega)$ be guarded by the map v and consider the family $\{A(r) : r \in U\}$. Then the set C defined by:

$$C = \{r \in \mathbb{R}^k : v(r) = v_\Omega(A(r)) = 0\} \quad \dots(14)$$

divides the parameter space \mathbb{R}^k into components C_i that are either stable or unstable relative to Ω . To see which situation prevails, one has to test $A(r)$ for any vector in C_i .

Supprimé : \mathbb{R}^k

Example 3: Damping region

Let ζ be a desired limiting minimum damping ratio (e.g. $\zeta = 0.707$). This leads to the region of generalized stability Ω_ζ (Fig. 7).

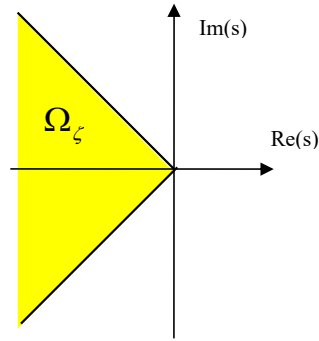


Figure 7. Damping region Ω_ζ

The guardian map corresponding to this region is given by

$$v(A) = \det(A^2 \circ I - (2\zeta^2 - 1)(A \circ A)) \det(A) \dots (15)$$

Suppose that the closed-loop poles of a given system are specified by the polynomial :

$$p(s) = s^3 + k_1 s^2 + k_2 s + k_3$$

where k_1, k_2, k_3 denote the controller gains. For the sake of visualization (see Fig. 7), let us fix the value of one of the gains, say $k_3 = 1$. Then one obtains (e.g. by applying (15) to the companion matrix corresponding to p , though this is not necessary):

$$v(p) = 2k_2^3 - k_1^2 k_2^2 - 4k_1 k_2 + 2k_1^3 + 1$$

Setting this quantity to 0, yields the 3 components of Fig. 8. It can be verified that the set of all gains (k_1, k_2) which place the closed-loop poles within the damping zone above is the top-right component. Any other choice of the gains yields closed-loop poles outside Ω . Indeed, this is so since the roots of p corresponding to, say $(k_1, k_2) = (5, 5)$, $(0, 0)$ and $(-5, -5)$, are respectively inside, outside and outside of Ω .

We end this section by stating that a systematic way of constructing guardian maps may be found in Saydy⁽⁵⁾.

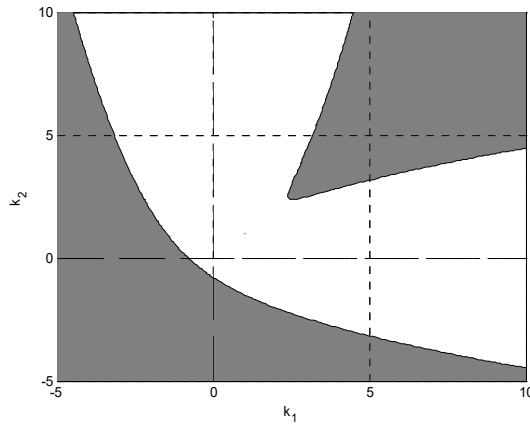


Figure 8. Set of all gains ensuring a certain damping ratio

5.0 PROPOSED APPROACH

Once the control structure has been fixed, the values of the 4 gains (K_q , K_p , K_i , K_{ff}) and the wash-out filter pole $-z_{wo}$ are to be chosen in an efficient way (Fig. 2). Modal and frequency criteria will be set up in two different ways. Model reduction and Guardian Maps are used to set the Short Period damping, whereas the frequency criteria are dealt with computationally, due to their more complex nature.

Supprimé : The

Supprimé : being

Supprimé : The dropback formula will be useful to express its value, depending on the gains retained.

The SAS loop is first tuned with the objective to make the Short Period modes sufficiently damped; this entails choosing appropriate values for K_q and $-z_{wo}$. Then, the designer may proceed to the choice of the three remaining CAS gains in order to finish the design. As it will be proved later, the dropback only depends on the K_i and K_{ff} gains for the control structure under consideration.

The methodology is applied to the longitudinal model of a business jet aircraft with the objective to track pitch-rate commands with predicted good level 1 handling qualities and desired time domain response (see Table 1).

The flight condition considered in this application is shown in Table 2.

Table 2 : Flight Condition in straight and level flight

Mach Number	Altitude	Dynamic Pressure
0.5	5000 ft	308.6 psf

First, we will present the reduction method that is used and how guardian maps were applied to set the Short Period damping. Then, the dropback formula will be established, followed by the computational methods used to set the frequency criteria.

5.1 Open loop model reduction

In order to practically use guardian maps, one has to reduce the system order; otherwise the computation time is prohibitive, as is always the case with general robustness methods dealing with parametric uncertainty. Moreover, only Short Period modes present a true interest; therefore, it is sufficient to obtain a reduction of this mode and the poles around it, in particular, the dominant actuator pole.

The objective that is sought is to make the Short Period modes of the global closed-loop system as close as possible to the Short Period modes that are assigned by control, based on the reduced-order system. This can be achieved by ensuring that the region found by guardian maps on the reduced model is similar to the one obtained for the high-order model.

Several order reduction methods (frequency reduction, modal truncation, balanced reduction, Hankel approximation) have been tested, and a mixed method has been selected.

First, the open-loop is simplified by gathering all the different pure delays coming from actuators and sensors, and by applying a Pade approximation on the resulting single delay. The system order is then lowered from a 35th to a 16th order. Then, as only the Short Period mode is at stake, we truncate the Phugoid mode by cancelling the u and θ states. The reduced system is then obtained by balancing the system with Matlab's[®] function `balreal` and by reducing the state vector using singular perturbation methods with the `modred` function.

Figure 9 shows the low-frequency pole-zero map of the considered 35th order open loop θ/δ_e for the design case. The poles we are interested in are: the Phugoid mode, the short period mode, the pole associated with the fifth state and the dominant actuator pole (not shown in the figure). All other system poles are much faster and do not interfere in the low frequency dynamics we consider for feedback. One could remark that the fifth pole due to the x_5 state is close to a system zero. In fact, this is the case for all trimmed models provided by *Bombardier Inc* at different flight conditions.

Supprimé : to

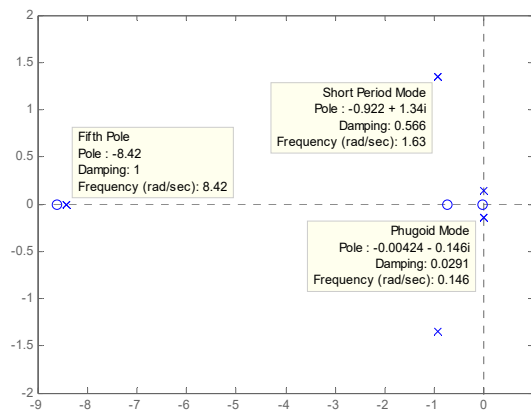


Figure 9. Pole/zero map (θ / δ_e)

After some trials, a 5th order reduction of q_{meas}/δ_c yields sufficiently close behaviours between the high-order and the low-order system after loop closure. One obtains the following order-reduced transfer function:

$$\left. \frac{q_{meas}}{\delta_c} \right)_{red} = \frac{0.001166s^5 - 0.07716s^4 + 3.6534s^3 + \dots}{s^5 + 47.67s^4 + 1195.12s^3 + \dots} \dots(16)$$

$$\frac{\dots - 105.50s^2 + 1444.29s + 2361.50}{\dots + 13197.90s^2 + 48348.05s + 135906.25}$$

Figure 10 shows that the HOS and LOS Bode diagrams compare favourably in the 0 to 20 rad/s frequency range of interest.

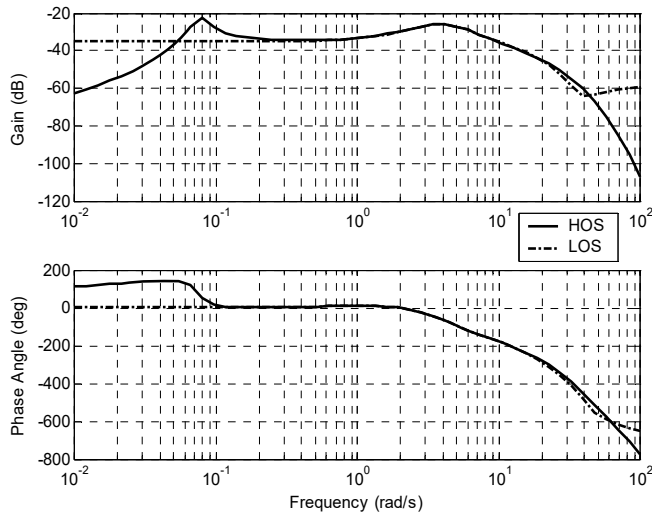


Figure 10. HOS and LOS Bode diagram comparison

A similar reduction procedure is carried out for the $n_{z,meas}/\delta_c$ transfer function:

$$\left. \frac{n_{z,meas}}{\delta_c} \right)_{red} = \frac{0.00415s^5 - 0.0357s^4 + 13.25s^3 + \dots}{s^5 + 47.67s^4 + 1195.12s^3 + \dots} \dots(17)$$

$$\frac{\dots - 152.40s^2 - 3098.18s + 40295.21}{\dots + 13197.90s^2 + 48348.05s + 135906.25}$$

5.2 Damping Set-Up

Guardian maps are now used to find gain parameter regions within which any choice of the gains will ensure that the closed-loop poles remain in a domain Ω similar to the one in Fig. 7. To be level 1, Phugoid and Short Period dampings must be above certain values. Even if Phugoid damping could easily be handled with Guardian Maps, it will not be treated here as it is not as crucial as the Short Period damping.

Remark: It should be noted that once the loops are closed there is no longer only one Short Period mode but there may be one, two or even three Short Period modes. Indeed, because of the filters and the dominant pole of the actuator, there may appear new complex modes whose natural frequency and damping could be considered as Short Period ones. It will be shown later how to handle this issue. Sensor poles are too fast to interfere if they have high frequency characteristics.

Supprimé : and

The main open loop transfer functions are (refer to Fig. 10):

$$\frac{q_{meas}}{\delta_c} = \frac{N_1(s)}{D(s)}, \quad \dots(18)$$

$$\frac{n_{z_{meas}}}{\delta_c} = \frac{N_2(s)}{D(s)}. \quad \dots(19)$$

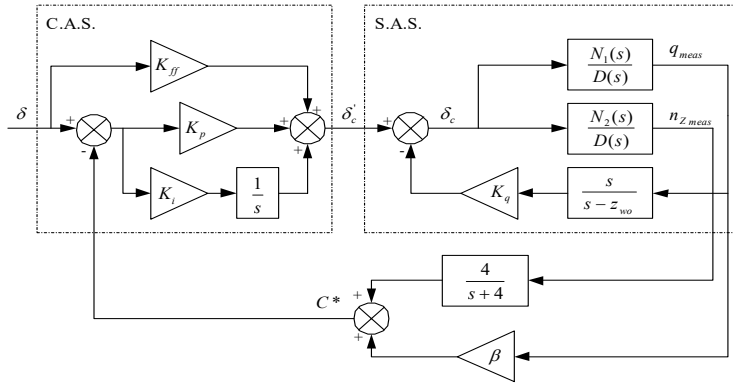


Figure 11. C* control law

According to Fig. 11, the SAS transfer function is then:

$$\frac{q_{meas}}{\delta'_c} = \frac{N_1(s)(s - z_{w0})}{D(s)(s - z_{w0}) + K_q s N_1(s)}. \quad \dots(20)$$

With $\beta=12.4$, one also has:

$$\frac{C^*}{\delta'_c} = \beta \frac{q_{meas}}{\delta'_c} + \frac{4}{s+4} \frac{n_{z_{meas}}}{\delta'_c} \quad \dots(21)$$

$$\begin{aligned} \frac{C^*}{\delta'_c} &= \frac{(s - z_{w0})(\beta N_1(s)(s+4) + 4N_2(s))}{(s+4)(D(s)(s - z_{w0}) + K_q s N_1(s))} \quad \dots(22) \\ &=: \frac{N_3(s)}{D_3(s)} \end{aligned}$$

Thus, in closed-loop,

$$\frac{C^*}{\delta} = \frac{((K_{ff} + K_p)s + K_i)N_3(s)}{sD_3(s) + (K_p s + K_i)N_3(s)} \quad \dots(23)$$

The K_{ff} gain does not modify the system poles. We therefore have at our disposition 4 parameters to place the poles. In a practical use of the methodology, it would be impossible to visualize the four parameter

subspaces. For this reason, damping set-up will be done in two steps: first the SAS is tuned, then the CAS design.

5.2.1 SAS design

SAS design is carried out by choosing K_q and the $-z_{wo}$ pole. This first loop is closed by placing the poles with a damping ratio of 0.7. Root locus analysis with wash-out filter feedback shows that the dominant actuator pole interacts with the natural poles.

To characterize the set of parameters K_q and $-z_{wo}$ which ensure the desired damping, a guardian map associated to the “damping” region Ω_ζ of Fig. 7 is used on the family of polynomials given by the denominator of the closed-loop SAS transfer function of (Eq. 20). Namely,

$$p(s) := D(s)(s - z_{wo}) + K_q s N_1(s),$$

which is a polynomial in s , the coefficients of which depend on the parameters K_q and $-z_{wo}$.

From the theory in Section 4, we can draw the set

$$C = \{(K_q, z_{wo}) \in \mathbb{R}^2 : V_{\Omega_\zeta}(p) = 0\}$$

to divide the space of parameters into regions of stability/instability relative to Ω_ζ .

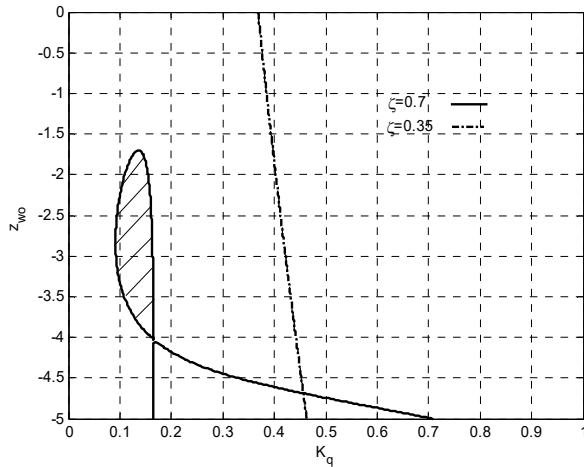


Figure 12. Guardian map zone for SAS loop

Figure 12 illustrates two drawings: the 0.7 and 0.35 damping ratio zones. In this case, choosing a couple $(K_q, -z_{wo})$ inside the dashed loop ensures that all the resulting poles will have a damping ratio greater than 0.7. Outside of this loop, at least one complex pair will have a damping ratio smaller than 0.7 but greater than 0.35 as long as $(K_q, -z_{wo})$ is to the left of the damping ratio line $\zeta = 0.35$. For every chosen pair, the GUI shows simultaneously the closed-loop poles. Let us take $K_q=0.11$ and $z_{wo}=-2.8$.

Remark:

To further corroborate the reduction effectiveness, we close the SAS loop on the high order system and compare the four dominant closed-loop poles with those of the reduced order system. Table 3 shows that the eigenvalue assignment is reasonably well conserved.

Table 3 : Closed-loop pole comparison after SAS feedback

HOS Poles	LOS Poles
-3.16±2.30i ($\zeta=0.808, \omega_n=3.91$)	-3.16±2.44i ($\zeta=0.791, \omega_n=3.99$)
-5.20±2.88i ($\zeta=0.875, \omega_n=5.94$)	-4.42±2.76i ($\zeta=0.918, \omega_n=5.99$)

5.2.2 CAS design

Once the SAS design is done, one gets a sixth order transfer function. With the n_z noise filter, the C^*/δ'_c transfer function (Eq. 22) is a 7th order one. We proceed in the same way as before: draw the guardian map (Fig. 13) and characterize the set of all pairs (K_p, K_i) which ensure the desired damping, namely the dashed region.

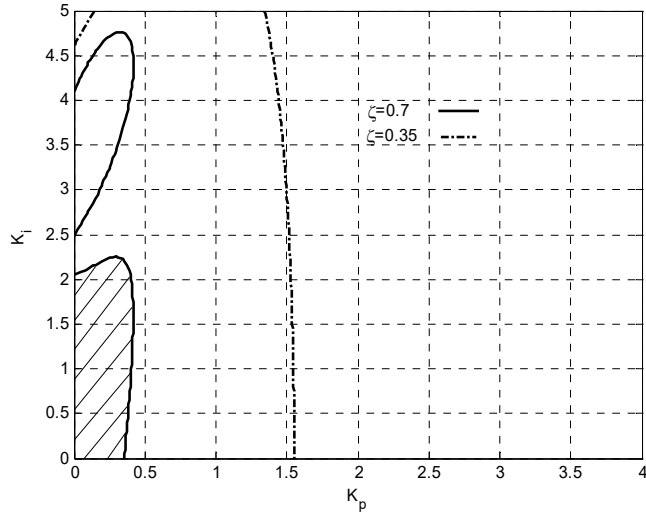


Figure 13. Guardian map zone for CAS loop

At this stage of the design, we have a characterization of all pairs (K_p, K_i) which satisfy the damping criteria.

This freedom of choice will now be exploited to satisfy the rest of the handling qualities.

5.3 Other criteria selection

Since the remaining handling qualities are not directly taken into account by the guardian map approach, a different way to include them is proposed. For the dropback criterion, the analytical formula in the system gains (Eq. 10) is used. For frequency criteria, the high order system is considered and a computational method is developed.

5.3.1 Dropback criterion

Combining (Eqs. 10 and 23), one is able to express the dropback in terms of the system gains:

$$Drb = \frac{K_{ff} - a}{K_i} + b \quad \dots(24)$$

where a and b are constants depending on the flight case. Note that K_q , K_p , or $-z_{wo}$ do not contribute to the dropback.

For our application and the flight condition under consideration, we obtain:

$$Drb = \frac{K_{ff} - 1.9502}{K_i} + 0.6149. \quad \dots(25)$$

Imposing limits D_{min} and D_{max} on Drb implies the following limits on K_{ff} :

$$(D_{min} - b)K_i + a < K_{ff} < (D_{max} - b)K_i + a. \quad \dots(26)$$

Supprimé : ones

For each dropback limiting value, the corresponding lines are drawn in Fig. 14. Thus all the (K_{ff}, K_i) pairs between the lines $Drb = 0$ and $Drb = 0.3$ fulfil the desired dropback requirement.

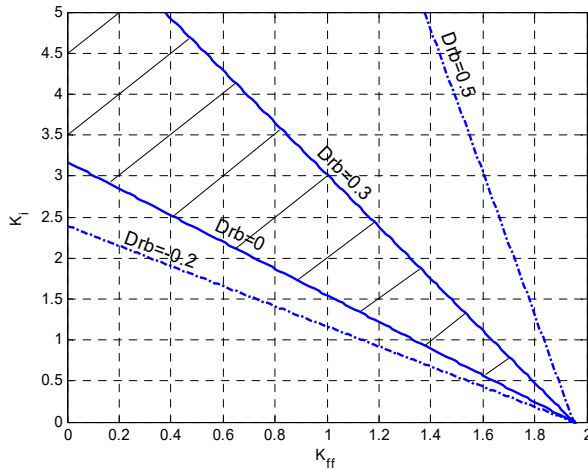


Figure 14. Dropback zone

The gain K_{ff} is chosen to be 0.6. This value ensures a satisfactory dropback (close to 0) for the maximum allowed K_i value of 2.1 (see Fig. 13). Indeed, a higher value of K_{ff} would provide better dropback but will result in a large overshoot.

5.3.2 Frequency response criteria

Now that K_{ff} is fixed, frequency response criteria are dealt with by tuning the gains K_p and K_i . For a given frequency criterion, we proceed in a manner similar to guardian maps to find all PI controller gains which satisfy a given frequency criterion; with the difference that this is done computationally. For instance, we find (K_p, K_i) that result in a 1.5 (rad/s) θ -bandwidth precisely. Once this boundary line found, the (K_p, K_i) space is divided into components where the θ -bandwidth criterion is or is not satisfied. We use a fixed controller grid and calculate for every one of the points in the grid, the different frequency criteria and plot the corresponding boundary. Although the approach is strictly computational, the algorithm is optimized to deliver very fast and accurate results. On a 1.5 GHz Centrino processor with 512 Mo RAM, all the frequency criteria are plotted within 20 seconds.

Figure 15 shows the superposition of all these criteria and the (K_p, K_i) zone that simultaneously fulfills all the requirements. The damping ratio 0.7 zone obtained with guardian maps has been superimposed.

The zone that satisfies all the handling quality criteria is the dashed one. Note that choosing poles with a minimum damping ratio of 0.7 generally fulfills most of the other criteria. Note also that there is no γ -bandwidth drawing as it is always satisfied.

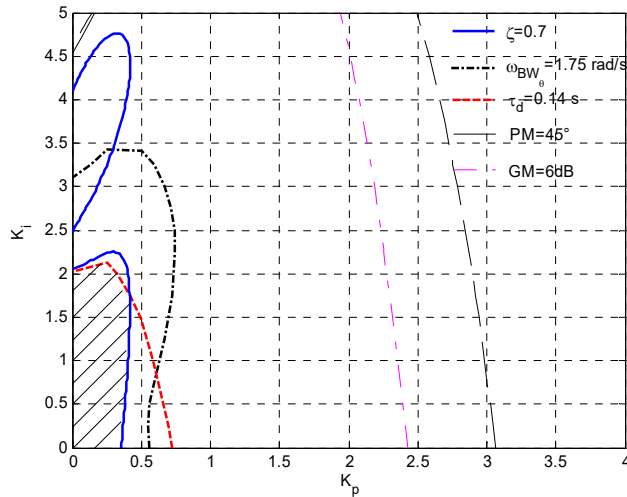


Figure 15. Handling quality drawing

A GUI is used to assist the designer through the different steps, which can display all the handling quality values for each targeted pair, as well as the desired time-responses: one can then find an adequate time-response in the zone. The chosen pair is $K_p=0.1$ and $K_i=1.9$.

Supprimé : and

Figure 16 illustrates the time-responses of interest: normalized pitch rate q (deg/s), pitch attitude θ (deg) and the mixed output C^* . These are the time responses without Phugoid mode dynamics.

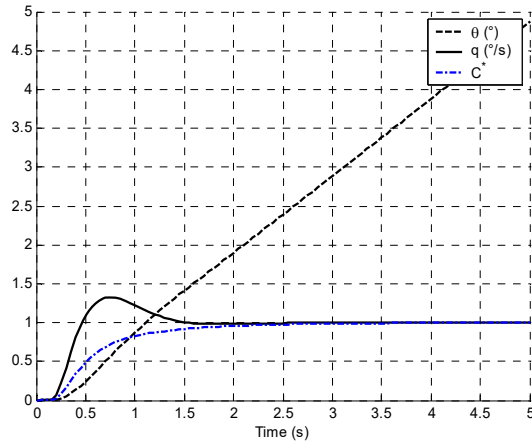


Figure 16. Time responses to a stick unit step

As was done before, Table 4 shows the reduction effectiveness as the placed closed-loop poles on the reduced system are close to the true placed closed-loop poles of the high-order system feedback.

Table 4 : Pole-Zero comparison after CAS loop feedback

HOS Poles	LOS Poles
-1.33	-1.35
$-2.52 \pm 1.82i$	$-2.55 \pm 1.77i$
$(\zeta=0.811, \omega_n=3.10)$	$(\zeta=0.821, \omega_n=3.11)$
$-3.28 \pm 3.19i$	$-3.22 \pm 3.16i$
$(\zeta=0.717, \omega_n=4.58)$	$(\zeta=0.714, \omega_n=4.51)$
-7.70	-8.29

Finally, Table 5 sums up the handling quality values for the given case, as well as the targeted limits.

Table 5 : Handling quality final values

HQs	Achieved	Level 1	Good Level 1
ζ_{ph}	>1.00	>0.04	
ζ_{sp1}	0.81	>0.35	>0.7
ζ_{sp2}	0.72	>0.35	>0.7
ζ_{sp3}	>1.00	>0.35	>0.7
$\omega_{BW\theta}$	2.60	>1.5 (rad/s)	>1.75 (rad/s)
$\omega_{BW\gamma}$	1.09	>0.6 (rad/s)	
τ_p	0.138	<0.2 (s)	<0.14 (s)
DrB	-0.0957	-0.2 < . <0.5	0.0 < . <0.3
Osh	32.41%		
ST	2.30	<3 (s)	
M_G	16.35	>6 (dB)	
$M\varphi$	74.36	> 45 (°)	

Supprimé : Current

Supprimé : Ideal

Remark:

As explained above, for every chosen flight condition, one can obtain gain subspaces where the handling qualities are all satisfied. Gain-scheduling aims at finding functions that will interpolate the gains found for each flight condition. The scheduling variable could be the dynamic pressure or some other variable such as altitude or Mach number.

The guidelines presented in this paper help with the gain scheduling process. Indeed, with this approach, gain scheduling boils down to finding interpolating functions that pass through these particular gain subspaces⁽³⁾.

5.4 GUI

As mentioned before, a graphical user interface was used to help obtain the results in this article. The GUI was developed on the MATLAB platform with MAPLE interactions to handle computer-algebra manipulations, in particular, to compute guardian map expressions. Figure 17 is a snapshot of one instance of utilisation, namely the one used to produce the results above.

Supprimé : s

Essentially, the GUI is comprised of six distinct areas which correspond to:

1. Model loading and order reduction
2. Ω -region and HQ selection
3. Time-response simulations and natural mode information
4. Controller gains selection, closed-loop poles and HQ information
5. Time-domain simulations plotting area
6. Guardian maps-based gain characterization plotting area (SAS or CAS)

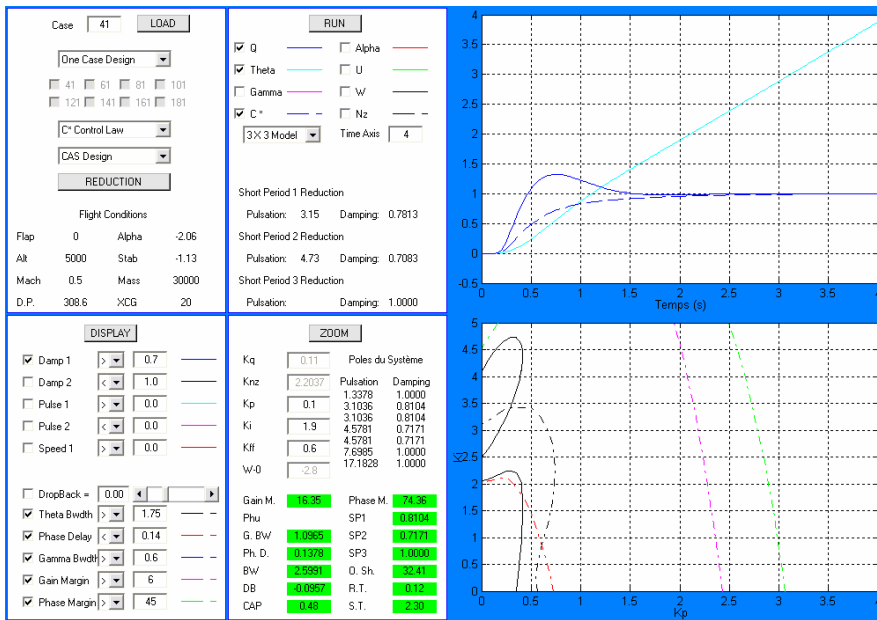


Figure 17. Graphical User Interface

6.0 CONCLUSION

This article presents guidelines to adjust the gains of a C^* control law while satisfying handling quality criteria. The pole damping requirements are fulfilled by using the guardian map theory. A theoretical dropback formula has been established which can be expressed in terms of the system gains. Frequency criteria are solved by computational methods. A GUI was developed and assists the designer in the design.

The application on a flight condition shows that the proposed method produces useful results. Moreover, the method can be used to achieve gain-scheduling through the whole flight envelope.

ACKNOWLEDGEMENTS

This work was funded by NSERC and *Bombardier Aerospace Inc.* under Grant CRD 215 465-98. The authors would like to thank Fraser MacMillen, David Reitz and Navid Niksefat of *Bombardier Aerospace Inc.* for their constructive remarks.

REFERENCES

1. Saydy, L., Akhrif, O. and Zhu, G. Handling Quality Characterization of Flight System Controller Gains, *Conference on Electronics, Circuits and Systems*, 2000, **2**, pp. 721-724.
2. Saussié, D., Saydy, L. and Akhrif, O. Flight Control Design with Robustness and Handling Qualities Requirements, *Electrical and Computer Engineering, IEEE CCECE Montreal*, 2003, **3**, pp. 1749-1752.
3. Saussié, D., Akhrif, O. and Saydy, L. Robust and scheduled longitudinal flight control design with handling quality requirements, *AIAA Guidance, Navigation, and Control Conference and Exhibit*, San Francisco, CA; United States; 15-18 Aug. 2005.
4. Saussié, D. Méthodologie pour le contrôle longitudinal d'un avion avec contraintes de qualités de manœuvrabilité, Mémoire de M. Sc A. , École Polytechnique de Montréal, 2004.
5. Saydy, L., Tits, A.L. and Abed, E.H. Guardian Maps and the Generalized Stability of Parametrized Families of Matrices and Polynomials, *Mathematics of Control, Signals and Systems*, 1990, **3**, pp. 345-371.
6. Gibson, J.C. *The Definition, Understanding and Design of Aircraft Handling Qualities*, Delft University Press, 1997
7. Hodgkinson, J. *Aircraft Handling Qualities*, AIAA Education Series, 1999.

8. Mitchell, D.G., Doman, D.B., Key, D.L., Klyde, D.H., Leggett, D.B., Moorhouse, D.J., Mason, D.H., Raney, D.L. and Schmidt, D.K. Evolution, Revolution, and Challenges of Handling Qualities, *Journal of Guidance, Control and Dynamics*, January-February 2004, **27**, (1), pp 12-28.
9. Kron, A., De Lafontaine, J. and Alazard, D. Robust 2-DOF H-infinity controller for highly flexible aircraft: Design methodology and numerical results, *Canadian Aeronautics and Space Journal*, Vol. 49, No 1. 2003. pp 19-29.
10. Puyou, G. and Chiappa, C. A multiobjective method for flight control law design, *AIAA Guidance, Navigation, and Control Conference and Exhibit*, Providence, RI; United States; 16-19 Aug. 2004. pp. 1-11. 2004
11. Tokutake, H., Sato, M. and Satoh, A. Robust Flight Controller Design That Takes into Account Handling Quality, *Journal of Guidance, Control and Dynamics*, January-February 2005, **28**, (1), pp 71-77.
12. Etkin, B. and Reid, L.D. *Dynamics of Flight: stability and control*, John Wiley & Sons, Inc., 1996.
13. McLean, D. *Automatic Flight Control Systems*, Prentice Hall International (UK) Ltd., 1990.
14. McRuer, D., Ashkenas, I. and Dunstan, G. *Aircraft Dynamics and Automatic Control*, Princeton University Press, 1973.
15. Tischler, M.B. *Advances in Aircraft Flight Control*, Taylor & Francis, 1996.
16. Field, E., The Application of a C* Flight Control Law to a Large Civil Transport Aircraft, Technical Report No 9303, College of Aeronautics, Cranfield Institute of Technology, 1993.
17. US Department of Defense. *Flying Qualities of Piloted Aircraft*, MIL-HDBK-1797, Washington: Government Printing Office 1997.

L'École Polytechnique se spécialise dans la formation d'ingénieurs et la recherche en ingénierie depuis 1873



École Polytechnique de Montréal

**École affiliée à l'Université
de Montréal**

Campus de l'Université de Montréal
C.P. 6079, succ. Centre-ville
Montréal (Québec)
Canada H3C 3A7

www.polymtl.ca

